Article

Tailoring a Behavioral Symmetry on KERMA, Mass Stopping Power and Projected Range Parameters against Heavy-Charged Particles in Zinc-Tellurite Glasses for Nuclear Applications

Lidya Amon Susam [1], Ayberk Yilmaz [1], Ghada ALMisned [2], Hatice Yilmaz Alan [3], Gizem Ozturk [1], Gokhan Kilic [4], Bahar Tuysuz [1], Selin Ece Topuzlar [5], Baki Akkus [1], Antoaneta Ene [6,*] and Huseyin Ozan Tekin [7,8,*]

1   Department of Physics, Faculty of Science, Istanbul University, Istanbul 34134, Türkiye;
    lidyamon@istanbul.edu.tr (L.A.S.); ayberk@istanbul.edu.tr (A.Y.); gizem.ozturk.2015@ogr.iu.edu.tr (G.O.);
    0452110031@ogr.iu.edu.tr (B.T.); akkus@istanbul.edu.tr (B.A.)
2   Department of Physics, College of Science, Princess Nourah Bint Abdulrahman University,
    Riyadh 11671, Saudi Arabia; gaalmisned@pnu.edu.sa
3   Institute of Nuclear Sciences, Ankara University, Ankara 06100, Türkiye; hyhaticeyilmaz@gmail.com
4   Department of Physics, Faculty of Science, Eskisehir Osmangazi University, Eskisehir 26040, Türkiye;
    gkilic@ogu.edu.tr
5   Department of Physics, Faculty of Science, Ege University, Izmir 35100, Türkiye; topuzlarselin@gmail.com
6   INPOLDE Research Center, Department of Chemistry, Physics and Environment, Faculty of Sciences and
    Environment, Dunarea de Jos University of Galati, 47 Domneasca Street, 800008 Galati, Romania
7   Department of Medical Diagnostic Imaging, College of Health Sciences, University of Sharjah,
    Sharjah 27272, United Arab Emirates
8   Computer Engineering Department, Faculty of Engineering and Natural Sciences, Istinye University,
    Istanbul 34396, Türkiye
*   Correspondence: antoaneta.ene@ugal.ro (A.E.); tekin765@gmail.com (H.O.T.)

Abstract: We present the behavioral changes and symmetrical enhancement on KERMA, mass stopping power and projected range parameters against heavy-charged particles through Indium (In) and Tantalum (Ta) incorporations for various zinc-tellurite glass groups such as TZI and ZTT for nuclear applications. SRIM and PAGEX codes are utilized for the determination of investigated attenuation parameters for alpha and proton particles. In KERMA calculations, the ZTT7 sample is reported to have the greatest release of charged particles because of an increase in kinetic energy. The mass stopping power values of all absorbent glass materials are steadily increased from 0 MeV to 0.1 MeV. TZI and ZTT attained their maximum mass stopping power at a kinetic energy value of 0.1 MeV. While comparable behavior patterns are seen for various energy values on the examined energy scale, the ZTT7 sample is observed with lower mass stopping power and projected range values against proton particles than the other samples. It can be concluded that zinc-telluride glasses through maximum Ta-reinforcement may be considered as promising materials for stopping the proton and alpha particles. Moreover, Ta-reinforcement may be considered as a monotonic tool in terms of providing a symmetry for attenuation enhancement against heavy-charged particles.

Keywords: heavy-charged particles; zinc-telluride glasses; SRIM; PAGEX; radiation protection

1. Introduction

The dose value and biological effect of different types of radiation are closely associated with LET and stopping power parameters. Charged particle's range means the distance to come to rest. The stopping power and projected range can be determined for protons (hydrogen ions) and α-particles (helium-ion) in different targets, such as carbon, air, water, calcium, iron, magnesium, silicon, aluminum, copper, graphite, etc. Heavy ions are used extensively in nuclear physics and industrial applications, accelerator technology, material surface research, radiotherapy, and ion implantation [1]. Bohr, Bethe and Bloch developed

a theory [2] to describe the energy loss of ions in solids, and this can be improved by many means including empirical and semi-empirical. There are many works performed on heavy ion interaction in different target materials, and these works give valuable information due to various ion beam-involved applications. The stopping powers of organic materials are also crucial for radiation physics applications in medicine, and in biology as well. A biocompatible material carbon is used in ion transport experiments due to its light mass; it is therefore most frequently used as a target element. Most of the publications show that to measure the ion energy loss by the transmission method, amorphous carbon targets and thin film graphite are prepared [3]. The ability of a medium to slow down charged particles is determined by the mean rate at which they lose energy at a certain location along their trajectory. The total stopping power is a function of both collisions stopping power and radiative stopping power. The typical rate of energy dissipation is due to inelastic scattering per unit of route length. The ability to prevent ionization and excitation of the medium's electrons due to Coulomb collisions is called the collision stopping power. The average energy loss per unit path length from the emission of bremsstrahlung is defined as the radiative stopping power. The stopping power is an important quantity because it helps us to understand the interactions between particle radiation types of ions with different energies and the target matter. The stopping power, range, energy loss, equivalent dose, and straggling are very significant parameters in many applications and research, such as radiation dosimetry, radiotherapy, health physics, medical physics, radiation chemistry, and nuclear physics. Stopping power is evaluated for charged particles, interacting with the material medium using a Coulombic method. The stopping power depends on the type of charged particle or projectile and the target material [4]. In addition to analytical methods to calculate these parameters, software was created for different purposes. One software package is SRIM (The Stopping and Range of Ions in Matter), which includes quick calculation, and calculates ion stopping, range in targets, sputtering, ion transmission, ion implantation, and ion beam therapy of ions in matter [5]. SRIM produces information on stopping powers, projected range and straggling distributions for any ion at any energy for elemental targets. More detailed calculations can be done, which show that it includes the targets with complex multi-layer configurations. SRIM packages have two parts for the stopping powers of high-energy (E > 1 MeV/u) heavy ions (Z > 3). The Brandt-Kitagawa approximation is used in one, while the multiple high-velocity effects are incorporated in the other, the Bethe-Bloch theory [6]. SRIM, which is based on Monte Carlo simulations, may be used to estimate how many ions will be deposited in materials after they have been bombarded by high-energy ions. Charged particle interactions and photon (X-ray and γ-ray) parameters may be calculated with the use of a program called PAGEX (interaction of Proton, Alpha, Gamma rays, Electrons, and X-rays with matter) [7]. Helium ion stopping power and range tables may be calculated in a variety of materials using the ASTAR software [8]. PSTAR is a software that determines the range and stopping power of protons in various materials [9]. Parameters for the density effect, range, stopping power, and radiation yield tables for electrons in various materials may be determined using the ESTAR software [10]. With these various codes, numerous literary treasures may be unearthed. In a previous study [11], Kurudirek examined heavy ions (H, C, Fe, Mg, Te, Pb, and U) and determined radiation damage and energy loss using the SRIM code at 100 keV kinetic energy. Ziegler et al. [6] have studied the energy loss and radiation damage in anthracene using the SRIM Monte Carlo code for 100 keV heavy ion irradiation. Yang et al. investigated the LET and beam spot width of the carbon ion beam in different heterogeneous phantoms [12]. MSP and PR are calculated for H^1 (proton particles) and He^{+2} (alpha particles) of La_2O_3 glasses with different software by Kilicoglu et al. [13]. Prabhu et al. developed software for calculating many parameters, such as mass attenuation coefficients, cross-sections, mass stopping powers of the charged particle, electron density, mass-energy absorption coefficient, effective atomic number, KERMA, and build-up factors for a wide energy range [14]. Using the MCNPX code, Kavaz et al. [15] calculated the mass attenuation coefficients (/) of CeO_2-doped barium bismuth borate

glasses in the 0.02–20 MeV range and compared their findings to those obtained using the WinXCOM program. Alpha particle and ion radiation interactions were explored by Ghossain, who determined the stopping power and range for several target materials, including bone, tissue, muscle, and water, at varying energies [2]. Scientists Inaniwa and Kanematsu looked at the ability to halt protons and helium, carbon, and oxygen ions [16]. Limiting entropy ratios for carbon ions were computed by Geithner et al. [17]. In another study, stopping power compilations were studied for alpha particle, proton, ^{12}C, ^{16}O, and ^{56}Fe for the target aluminum, copper, iron, and silicon [18]. In Correa's study, he explained in detail how the electronic stopping power in the materials was calculated [4]. Saadi and Machrafi developed a new code for calculating stopping power for the electron and positron [19]. Bake et al. [20] measured the stopping power of liquid water for carbon ions. The mass-stopping power of protons for the Pb and Be targets were calculated by Iqbal et al. [21]. Using the transmission technique, Crnjac A. et al. [3] calculated the proton energy loss through a single-crystal diamond membrane with a thickness of 3.5 m for energies between 1.6 MeV and 6 MeV. Diamond's braking power was calculated and compared to SRIM [3] based on the research conducted. Using glass for radiation fields has been a popular topic of discussion in recent years. This is because glasses and other glass products have exceptional optical, mechanical, and structural properties. Upon reviewing the literature, it is evident that glass materials hold a significant position in the field of space studies. The characterization of particle radiation for glass materials is of utmost importance, given that a substantial portion of cosmic radiation comprises such radiation. The efficacy of these glass solutions in the space environment is attributed to their ability to maintain a stable transmission of light, ranging from UV to near infrared, while exhibiting high UV radiation absorption, shielding against particle radiation, and possessing a low coefficient of thermal expansion. Additionally, these solutions are composed of lightweight materials. In a previous study, Palmer et al. investigated the potential applications of glass materials for spacecraft design and the potential applications of glass material for space applications [22].

In this research, parameters such as KERMA, mass arresting power, and predicted range against radiation types such as alpha and proton were examined. The main purpose of this study is to calculate the mass stopping powers, projected range, and KERMA for helium and hydrogen using twelve different zinc-tellurite glasses (TZI2, TZI4, TZI6, TZI8, ZT, ZTT1, ZTT2, ZTT3, ZTT4, ZTT5, ZTT6, ZTT7) reinforced by Indium (In) and Tantalum (Ta) between the 10 keV and 10 MeV energy range. The finding of the current investigation may be useful in terms of determining a monotonic tool for the enhancement of symmetrical behavioral changes toward better absorption properties against alpha and proton particles.

2. Materials and Methods

2.1. Theoretical Background

The stopping power of an ion beam can be calculated for a variety of energies and ion beam-target combinations using the principle that charged particles lose energy in a medium through collisions with orbital electrons of atoms (ionization and excitation) of the medium (collisional stopping power) and emission of radiation in the coulomb field of target nuclei (radiative stopping powers or bremsstrahlung) [19]. Particles with low electric charge suffer energy losses due to collisions and radiation. By exciting and ionizing atoms in the medium and losing energy this way, heavy-charged particles gradually but continuously lose energy. Collisions with target nuclei (nuclear stopping) and electrons (electronic stopping) cause ion beams to lose energy if they penetrate matter deeply [23]. As the kinetic energy of a charged particle decreases as it slows down, its stopping power is defined as $-\mathrm{d}E/\mathrm{d}x$.

$$-\frac{dE}{dx} = \frac{4\pi k_0^2 Z^2 e^4 n}{mc^2\beta^2}\left[\ln\frac{2mc^2\beta^2}{I(1-\beta^2)} - \beta^2\right] \tag{1}$$

The stopping power described as the mean energy loss per unit path length depends on the charge and velocity of the projectile and content of the target material [2].

2.2. SRIM and PAGEX Codes

The SRIM collection of programs may calculate ion-matter interactions, such as ion stopping and range in targets, ion transmission, implantation, ion beam treatment, and sputtering. The original programs were created by James F. Ziegler and Jochen P. Biersack in the early 1980s, and since then, there have been major updates to the software once every five years [24,25]. Using the binary collision approximation, in which the impact parameter of the next colliding ion is chosen at random [26–28], SRIM is founded on a Monte Carlo simulation strategy. The electronic stopping power was determined using an average of several trials. As an added bonus, the interatomic potential has been calculated using a universal form derived from quantum mechanical computations. The effects of radiation depend on the type and energy of the radiation in addition to the radiological properties of the irradiated medium, and thus, it is crucial to evaluate all radiation interaction parameters to effectively characterize the radiological properties of the medium. The PAGEX package is a versatile, cross-platform software solution that supports quick and efficient computations of photon (X-ray and γ-ray) and charged particle interaction parameters applicable to a variety of disciplines [14]. It is based on proven theoretical formulations and calculations, connecting Python libraries for computing quantities such as charged particle cross-sections, mass stopping powers, and KERMA across a broad energy range. SRIM and PAGEX are well-known in the area of ion implantation research and technology, as well as in many other radiation material science domains.

2.3. Investigated Glass Samples

In this study, the mass stopping power and projected range characteristics of zinc-tellurite glasses with various additive types and ratios [29,30] were investigated against heavy-charged particles. Sample codes, elemental mass fraction (wt.%), and densities are given in Table 1. Figure 1 depicts the physical appearances of ZTT and TZI glasses, respectively. Although the research team has examined some characteristic properties of these glasses in previous studies, the absorption properties of the materials against heavy-charged particles are uncertain, as are the conditions of use and penetration-response functions in applications where these types of radiation such as alpha and proton are present. This gap prompted the research team to undertake the current extensive investigation. TZI [29] and ZTT [30] glass groups were studied in this research. The TZI [29] glass group was synthesized for the first time in terms of its chemical configuration, and its optical (transmittance, absorption, optical band gap, Urbach energy), physical (density and molar volume), and gamma ray absorption characteristics were examined. On the other hand, the zinc-telluride glass series, which is referred to as the ZTT group, was synthesized by doping 0–7 mole% Ta_2O_5 to the structure, and structural (XRD and FTIR), thermal (the glass transition temperature (Tg), crystallization temperature (Tc), and thermal stability (ΔT)) data for eight samples were obtained. Optical (transmittance, absorption, optical band gap, Urbach energy, refractive index), physical (density and molar volume), and electrical (conductivity and resistivity) characteristics were examined.

Table 1. Sample codes, elemental mass fraction (wt.%), and densities.

Sample	Te	Zn	In	Ta	O	Density (g/cm³)
TZI2	29.210	4.467	1.375	0.000	64.948	5.60
TZI4	28.620	3.704	2.694	0.000	64.983	5.63
TZI6	28.053	2.970	3.960	0.000	65.017	5.65
TZI8	27.508	2.265	5.178	0.000	65.049	5.67
ZT	27.273	9.091	0.000	0.000	63.636	5.51
ZTT1	26.589	8.863	0.000	0.716	63.832	5.55
ZTT2	25.926	8.642	0.000	1.411	64.021	5.59
ZTT3	25.282	8.427	0.000	2.085	64.205	5.64
ZTT4	24.658	8.219	0.000	2.740	64.384	5.69
ZTT5	24.051	8.017	0.000	3.376	64.557	5.75
ZTT6	23.461	7.820	0.000	3.993	64.725	5.78
ZTT7	22.888	7.629	0.000	4.594	64.889	5.82

The header "Elemental Mass Fractions (wt.%)" spans the Te, Zn, In, Ta, and O columns.
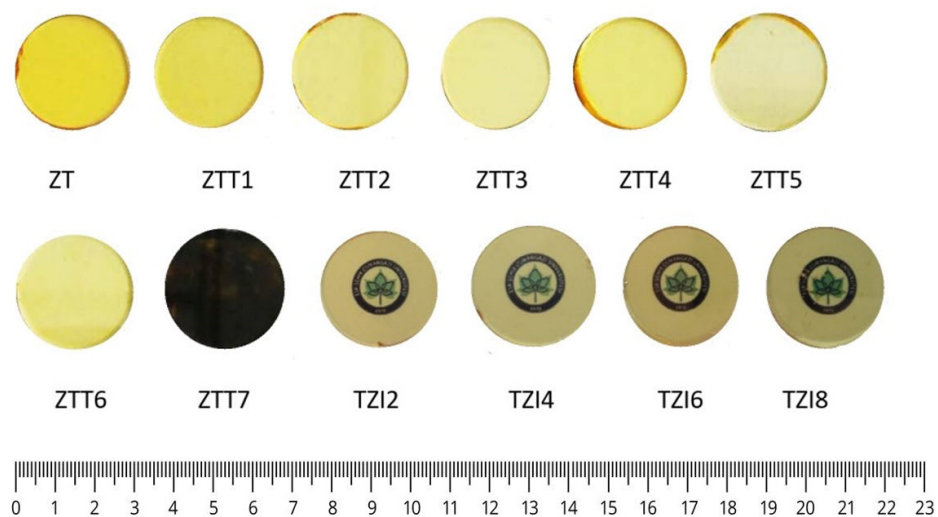
Figure 1. Physical appearances of investigated ZTT and TZI glasses.

3. Results and Discussion

3.1. Assessment of KERMA Values for Glass Shields

In radiation physics applications, knowing the KERMA value is very crucial. KERMA essentially describes the quantity of kinetic energy released by a substance. The KERMA value is the total kinetic energy of the charged particles produced by the interaction of uncharged ionizing radiation such as gamma rays and X-rays. There are two stages involved in the process of transferring photon energy to matter. Firstly, a variety of photon interactions transfer energy to charged particles in the medium. The secondary charged particles then use atomic excitation and ionization to release their energy into the surrounding medium. In this study, the KERMA values of some glass absorption materials of different elemental compositions were calculated in the kinetic energy range of 0–10 MeV. The fluctuation of the KERMA value as a function of increasing kinetic energy for each of the twelve examined glass samples is shown in Figure 2. With extremely low quantities of kinetic energy, the KERMA values are seen to be minimal. Nevertheless, the KERMA values, which started to increase at 0.004 MeV, initiated a more significant increasing trend at the 0.01 MeV kinetic energy value. The KERMA values, which started a strong increasing trend from a kinetic energy value of 0.01 MeV to a value of 0.05 MeV, reached a maximum

of 0.05 MeV. As a function of the rise in kinetic energy from 0.3 MeV to 10 MeV, the KERMA values, which followed a steeply descending trend after this value, assumed an average horizontal trajectory.
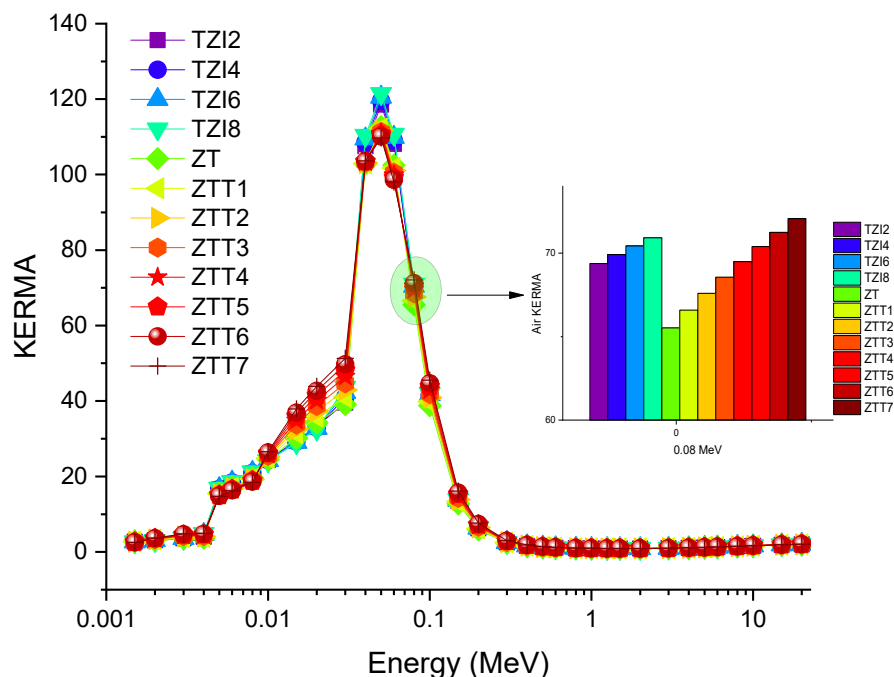

Figure 2. Variation of KERMA values for TZI and ZTT glasses at different kinetic energy values.

Considering the changing patterns of the KERMA values for the studied materials, it is evident that the ZTT7 sample has the highest kinetic energy values, except for the peak point. The KERMA value is the ratio of the mass absorption coefficient of the absorbent material to the mass absorption coefficient of the air, and it is represented by the equation below [31].

$$KERMA = ((\mu/\rho)_{compound})/((\mu/\rho)_{air})$$

Hence, it is anticipated that materials having a high photon mass absorption coefficient would have a high KERMA value. This may be explained by the fact that more energy is transferred per unit mass when a greater proportion of the input photon beam with a high absorption coefficient is removed. This rapid energy transfer also increases the excitation of charged particles within the absorber. Hence, the ZTT7 sample, which has the greatest mass absorption coefficient among the materials, is anticipated to have the highest KERMA values, given that the mass attenuation coefficient of air will remain constant throughout the KERMA calculation for each sample. This indicates that the ZTT7 sample might have the greatest release of charged particles as a consequence of an increase in kinetic energy. This behavior may be explained by the superior absorption of ZTT7, in which the greatest interaction in the sample results in the largest energy transfer to charged particles. As given in Table 1, ZTT7, which has a density value of 5.82 g/cm^3 and an elemental mass fraction value of 4.594 wt.%, demonstrates the best absorption capabilities based on the KERMA parameter.

3.2. Assessment of Mass Stopping Power Values for Glass Shields

Nuclear and materials physicists use the term stopping power to describe the force that acts to slow down charged particles, such as alpha and beta particles, as they contact matter and lose energy in the process. Radiation shielding, ion implantation, and nuclear medicine all benefit through its application. When they travel through matter, charged particles and neutrons in the nucleus both undergo energy dissipation. In many of the examples, positive ions are considered for the above-mentioned applications such as nuclear and material

physics. To what extent radiation is impeded by a given substance is determined by the nature of the radiation itself as well as the features of the medium through which it travels. In this work, the mass stopping powers for alpha and proton particles of the examined absorber glass materials for kinetic energies between 0 and 10 MeV were determined.

The mass stopping ability of TZI and ZTT glasses against protons bombarded with hydrogen as a function of increasing kinetic energy is shown in Figure 3. The mass stopping power of all absorbent glass materials has steadily increased from 0 MeV to 0.1 MeV, as seen in the figure. Glass materials, which attained their maximum mass stopping power at a kinetic energy value of 0.1 MeV, began to decrease as the kinetic energy value increased to 10 MeV. While comparable behavior patterns are seen for various energy values on the examined energy scale, the ZTT7 sample has a lower mass stopping strength against proton particles than the other samples. This is because ZTT7 provides the slowing procedure for protons with identical kinetic energies by using the lowest mass stopping power. Charged alpha particles extracted from the He nucleus exhibit a similar tendency. The mass stopping powers of ZTT and TZI glasses as a function of increasing kinetic energy are shown in Figure 4. Here, it can be shown that the acquired mass stopping capabilities surpass those of protons. This is due to the rigid mass differences between helium, which has an amu of 4.0026, and protons, which have an amu of 1.0072. In other words, the stopping power that must be shown against the kinetic energy is strongly connected to the particle mass that is attempting to be stopped. Nevertheless, the ZTT7 sample exhibited the lowest mass stopping power values against alpha particles, resulting in the most effective absorption condition. Calculating the stopping power of electrons crossing matter is comparable to calculating the stopping power of heavy-charged particles.
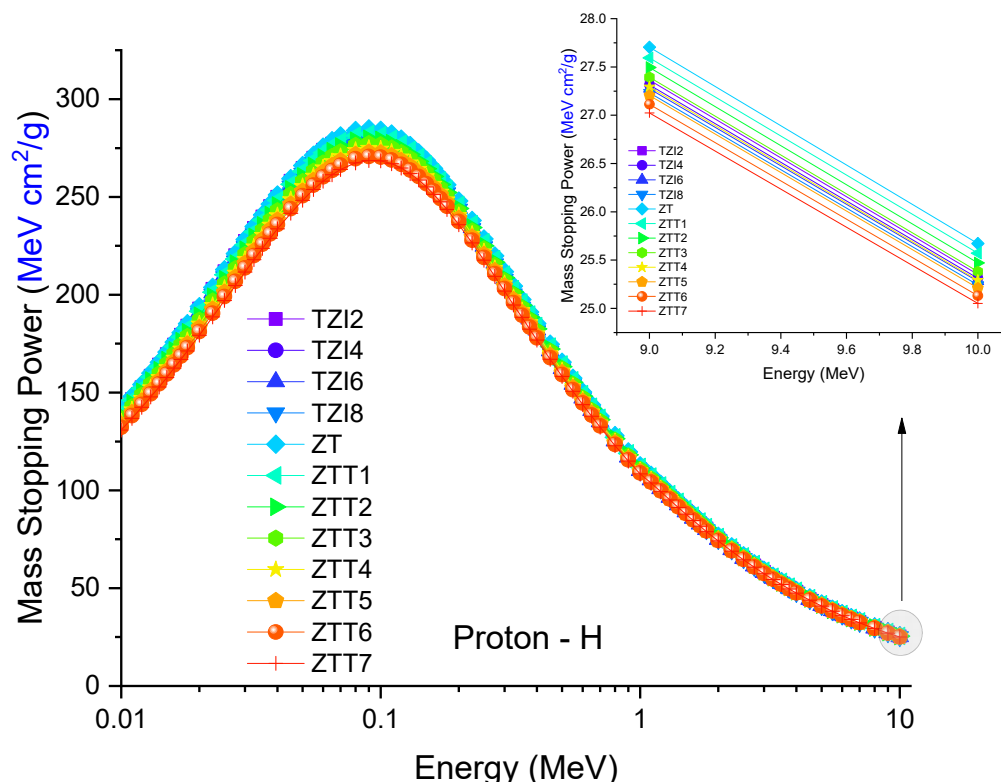

Figure 3. Variation of proton mass stopping power values for TZI and ZTT glasses at different kinetic energy values.
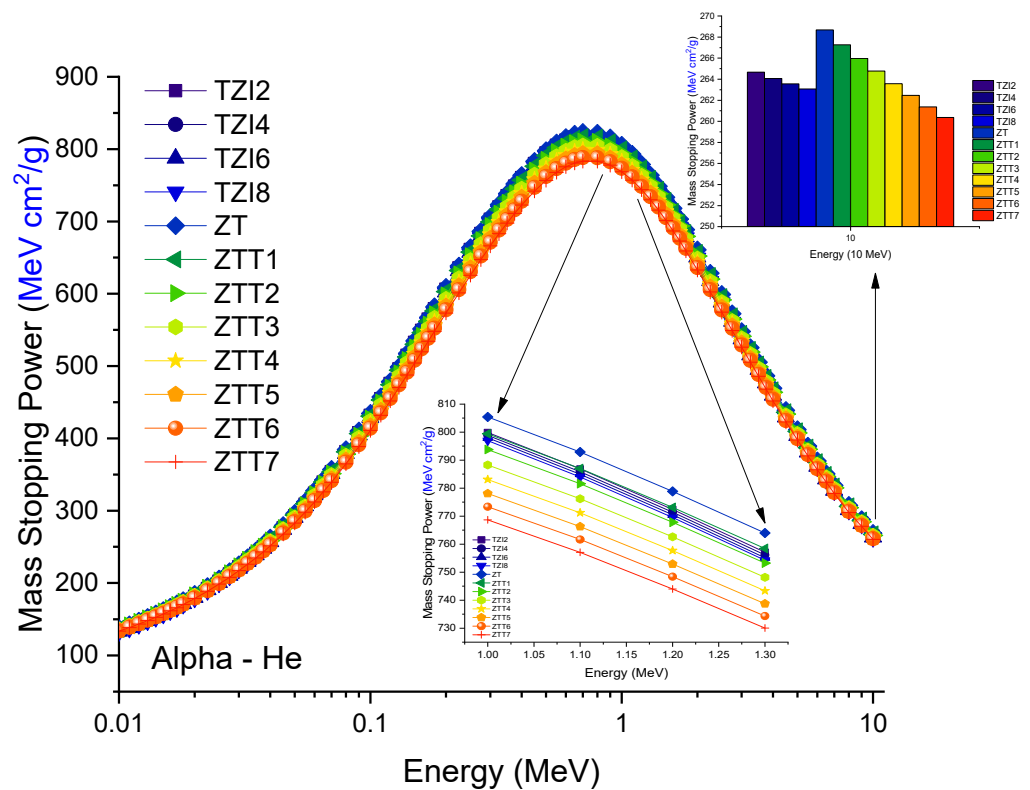
Figure 4. Variation of alpha mass stopping power values for TZI and ZTT glasses at different kinetic energy values.

Bethe's theory may be used to calculate the collisional stopping power, which is the interaction between incoming electrons and atomic electrons that leads to excitation and ionization. Bremsstrahlung, or electromagnetic radiation, is also produced when electrons are accelerated in the Coulomb field of nuclei. Figure 5 presents the kinetic energy-dependent variation of the resulting mass stopping power for electrons. Mass stopping power superiorities obtained for alpha protons were obtained with ZTT7 sample superiority for electrons. This can be explained by the fact that the mass arresting force in principle exhibits similar behavior for charged particles. In nuclear physics, another important parameter for charged particles is known as projected range. The projected range is the average depth to which a charged particle would penetrate as it slows down and comes to rest. Its depth is measured along the particle's starting direction. As a result, the minimum projected range values for the materials indicate that the distance charged particles would travel before coming to rest in the material will likewise be minimal; this is an absorption advantage. In other words, materials having a smaller projected range value for proton or alpha with the same kinetic energy value absorb these charged particles more effectively. Figures 6 and 7 depict the variance in computed range values based on kinetic energy. As seen by the figures, the predicted range value for both protons and alpha particles increased as the kinetic energy value increased. In other words, the penetration of protons and alpha particles with high kinetic energy increased in the material, as it increased the lengths necessary for them to reach the rest state. Despite this, the predicted projected range values for hydrogen at the same kinetic energy levels are higher. This may be explained by hydrogen's lower mass relative to helium's. On the other hand, the short range of heavy helium particles in the material is reflected in the projected range values, and as shown in the figures, for the same kinetic energy values, lower projected range values are given to Helium particles.
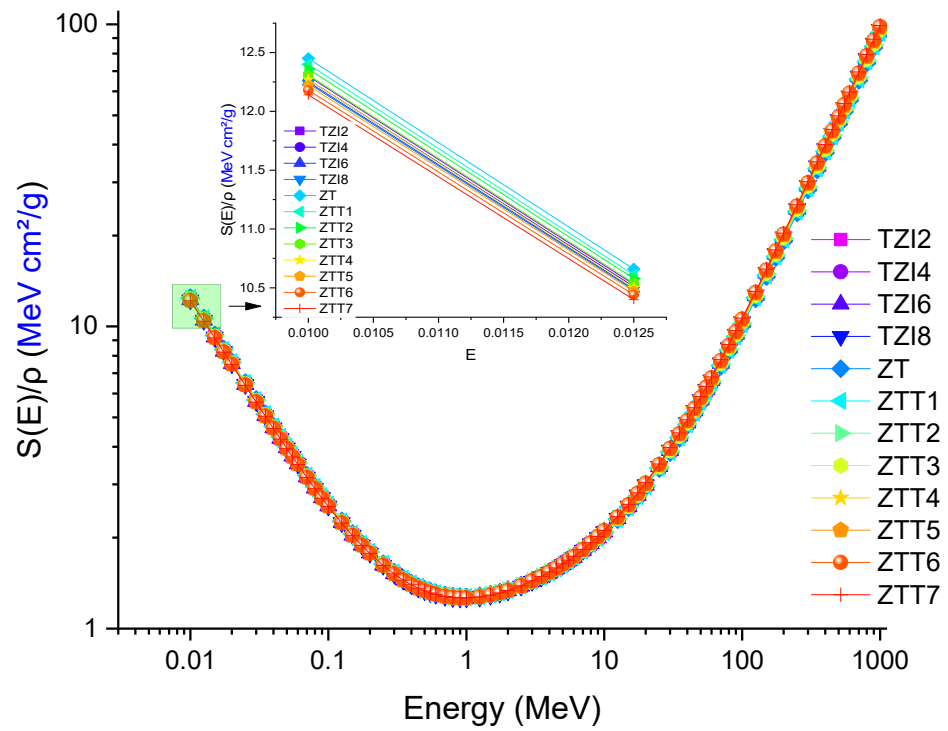
Figure 5. Variation of electron mass stopping power values for TZI and ZTT glasses at different kinetic energy values.
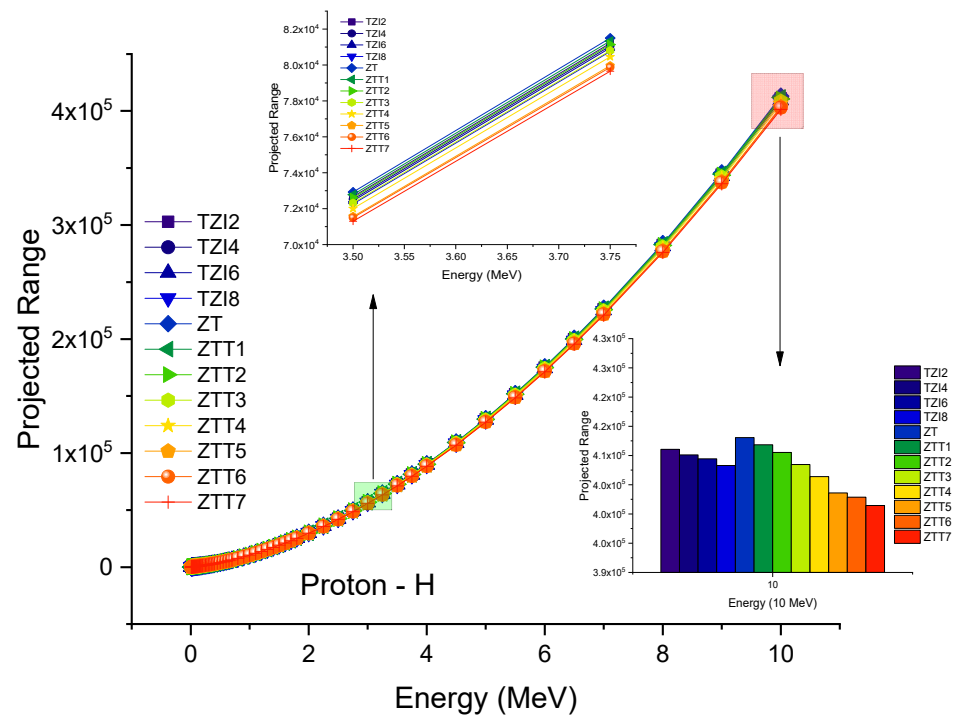

Figure 6. Variation of proton projected range values for TZI and ZTT glasses at different kinetic energy values.
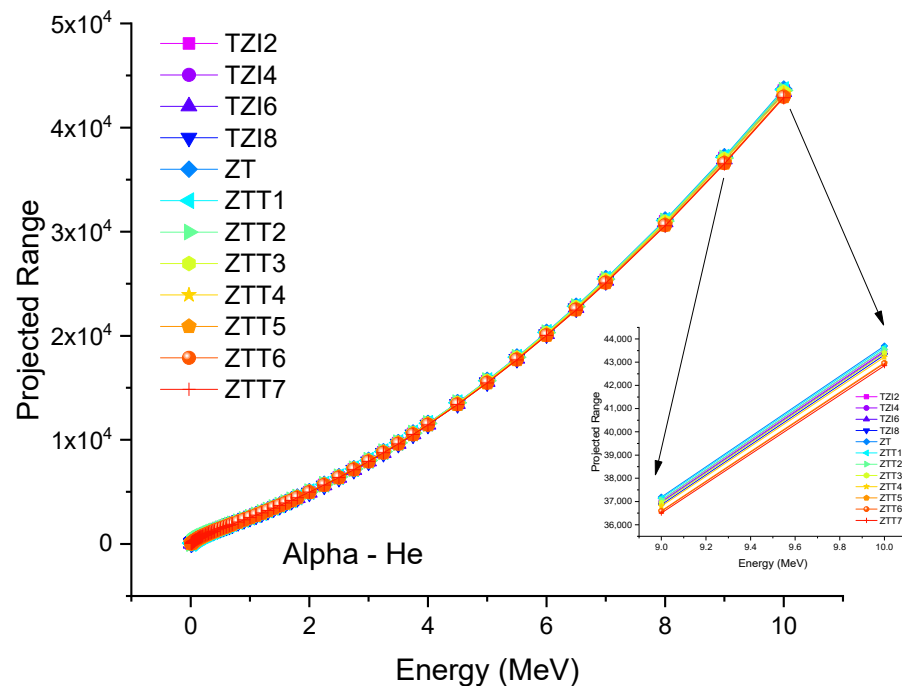
Figure 7. Variation of alpha projected range values for TZI and ZTT glasses at different kinetic energy values.

Nonetheless, the lowest predicted range values for both proton and alpha particles were found for the material with the maximum density ZTT7. This is a continuation of the better mass stopping power capabilities of ZTT7, delivering the shortest projected range against hydrogen and alpha particles, and accomplishing the transition to resting states at a specific kinetic energy value at the shortest distances. Likewise, among the tested glass materials, it is feasible to absorb charged particles with energies ranging from 0 to 10 MeV at the shortest distances and with the shortest projected range values.

4. Conclusions

Radiation is a form of energy that is both naturally and artificially existent. Depending on the amount of radiation exposure, many consequences may be detected in living biological tissue, including deterministic and stochastic effects. Shielding is the most significant component of the radiation protection principles, whose primary directions are specified by the ALARA (As Low As Reasonably Achievable) principle. This concept suggests that dose exposure and, therefore, radiation-induced health concerns may be minimized by using the most suitable absorber material based on the type and energy of radiation. In recent years, the use of glass materials for radiation fields has attracted considerable interest. This is because glass materials possess outstanding optical, mechanical, and structural qualities. In this research, parameters such as KERMA, mass arresting power, and predicted range against radiation types such as alpha and proton were examined. It has been determined that the chemical configuration of the glass structure has a direct impact on these critical parameters for the investigated glass TZI and ZTT groups. Due to the rise in In and Ta, the quantities of Te and Zn decreased in both glass groups. This alteration in reverse allowed the improvement of calculated parameters in both glass groups separately, and favorably impacted the TZI and ZTT glasses in the direction of superior heavy-charged particle absorption. Among TZI and ZTT glasses, it was reported that the ZTT7 sample with the highest Ta content has superior properties. Several essential material characteristics acquired by maximum Ta doping in this sample have previously been published, and based on the results of this investigation, it can be concluded that the highest concentration of Ta that can be incorporated to zinc-telluride glasses may be utilized to produce behavioral symmetry for such glass structures.

References

1. Flerov, G.N.; Barashenkov, V.S. Practical applications of heavy ion beams. *Sov. Phys. Uspekhi* **1975**, *17*, 783–793. [CrossRef]
2. Ghossain, M.O. Calculations of Stopping Power, and Range of Ions Radiation (Alpha Particles) Interaction with Different Materials and Human Body Parts. *Int. J. Phys.* **2017**, *5*, 92–98.
3. Crnjac, A.; Jakšić, M.; Matijević, M.; Rodriguez-Ramos, M.; Pomorski, M.; Siketić, Z. Energy loss of MeV protons in diamond: Stopping power and mean ionization energy. *Diam. Relat. Mater.* **2023**, *132*, 109621. [CrossRef]
4. Correa, A.A. Calculating electronic stopping power in materials from first principles. *Comput. Mater. Sci.* **2018**, *150*, 291–303. [CrossRef]
5. SRIM - The Stopping and Range of Ions in Matter. Available online: http://www.srim.org/ (accessed on 15 January 2023).
6. Ziegler, J.F.; Ziegler, M.D.; Biersack, J.P. SRIM—The stopping and range of ions in matter. *Nucl. Instrum. Methods B* **2010**, *268*, 1818–1823. [CrossRef]
7. Available online: https://github.com/sriharijayaram5/PAGEX (accessed on 20 January 2023).
8. Available online: https://physics.nist.gov/PhysRefData/Star/Text/ASTAR.html (accessed on 15 January 2023).
9. Available online: https://physics.nist.gov/PhysRefData/Star/Text/PSTAR.html (accessed on 15 January 2023).
10. Available online: https://physics.nist.gov/PhysRefData/Star/Text/ESTAR.html (accessed on 15 January 2023).
11. Kurudirek, M. Effective atomic number, energy loss and radiation damage studies in some materials commonly used in nuclear applications for heavy charged particles such as H, C, Mg, Fe, Te, Pb and U. *Radiat. Phys. Chem.* **2016**, *122*, 15–23. [CrossRef]
12. Yang, S.; Zhao, J.; Zhuo, W.; Shen, H.; Chen, B. Changes of the linear energy transfer (LET) and beam width of therapeutic carbon ion beam in density heterogeneous phantoms. *J. Radiol. Prot.* **2022**, *42*, 021518. [CrossRef]
13. Kılıcoğlu, O.; Altunsoy, E.; Agar, O.; Kamislioglu, M.; Sayyed, M.; Tekin, H.; Tarhan, N. Synergistic effect of La$_2$O$_3$ on mass stopping power (MSP)/projected range (PR) and nuclear radiation shielding abilities of silicate glasses. *Results Phys.* **2019**, *14*, 102424. [CrossRef]
14. Prabhu, S.; Jayaram, S.; Bubbly, S.; Gudennavar, S. A simple software for swift computation of photon and charged particle interaction parameters: PAGEX. *Appl. Radiat. Isot.* **2021**, *176*, 109903. [CrossRef]
15. Kavaz, E.; Tekin, H.O.; Agar, O.; Altunsoy, E.E.; Kilicoglu, O.; Kamislioglu, M.; Abuzaid, M.M.; Sayyed, M.I. The Mass stopping power/projected range and nuclear shielding behaviors of barium bismuth borate glasses and influence of cerium oxide. *Ceram. Int.* **2019**, *45*, 15348–15357. [CrossRef]
16. Inaniwa, T.; Kanematsu, N. Effective particle energies for stopping power calculation in radiotherapy treatment planning with protons and helium, carbon, and oxygen ions. *Phys. Med. Biol.* **2016**, *61*, N542. [CrossRef]
17. Geithner, O.; Andreo, P.; Sobolevsky, N.; Hartmann, G.; Jäkel, O. Calculation of stopping power ratios for carbon ion dosimetry. *Phys. Med. Biol.* **2006**, *51*, 2279–2292. [CrossRef]
18. Vegena, E.; Androulakaki, E.; Kokkoris, M.; Patronis, N.; Stamati, M. A comparative study of stopping power calculations implemented in Monte Carlo codes and compilations with experimental data. *Nucl. Instrum. Methods Phys. Res. Sect. B Beam Interact. Mater. At.* **2020**, *467*, 44–52. [CrossRef]
19. Saadi, M.; Machrafi, R. Development of a new code for stopping power and CSDA range calculation of incident charged particles, part A: Electron and positron. *Appl. Radiat. Isot.* **2020**, *161*, 109145. [CrossRef] [PubMed]
20. Bake, W.Y.; Braunroth, T.; Rosales, L.D.L.F.; Rahm, J.M.; Rabus, H. Stopping power of water for carbon ions with energies in the Bragg peak region. *Phys. Rev. E* **2020**, *102*, 062418. [CrossRef]

21. Iqbal, A.; Ullah, N.; Rahman, A.U. Density-dependent Energy Loss of Protons in Pb and Be Targets and Percent Mass-Stopping Power from Bethe-Bloch Formula and Bichsel-Sternheimer Data within 1–12 MeV Energy Range: A Comparative Study Based on Bland-Altman Analysis. *J. Med. Imaging Radiat. Sci.* **2019**, *50*, 149–156. [CrossRef] [PubMed]
22. Palmer, G.; Bailey, B.; Wilkinson, C.; Duru, F. Radiation Shielding Capabilities of Glasses with Potential Applications in Spacecraft and Laboratories. In Proceedings of the APS March Meeting 2018 Volume 63, Number 1 Monday–Friday, Los Angeles, CA, USA, 5–9 March 2018.
23. Brandt, W.; Kitagawa, M. Effective stopping-power charges of swift ions in condensed matter. *Phys. Rev. B* **1982**, *25*, 5631–5637. [CrossRef]
24. Biersack, J.P.; Haggmark, L.G. A Monte Carlo computer program for the transport of energetic ions in amorphous targets. *Nucl. Instrum. Methods* **1980**, *174*, 257–269. [CrossRef]
25. Ziegler, J.F.; Ziegler, M.D.; Biersack, J.P. *The Stopping and Range of Ions in Matter*; Pergamon Press: New York, NY, USA, 1985; ISBN 978-0-08-021607-2.
26. Robinson, M.; Torrens, I. Computer simulation of atomic-displacement cascades in solids in the binary-collision approximation. *Phys. Rev. B* **1974**, *9*, 5008–5024, Bibcode: 1974PhRvB...9.5008R. [CrossRef]
27. Was, G. *Fundamentals of Radiation Materials Science*; Springer: Berlin/Heidelberg, Germany, 2013.
28. Smith, R. *Atomic & Ion Collisions in Solids and at Surfaces: Theory, Simulation and Applications*; Cambridge University Press: Cambridge, UK, 1997; ISBN 978-0-521-44022-6.
29. Kilic, G.; Ilik, E.; Issa, S.A.; Issa, B.; Issever, U.; Zakaly, H.M.; Tekin, H. Fabrication, structural, optical, physical and radiation shielding characterization of indium (III) oxide reinforced $85TeO2-(15–x)ZnO-xIn_2O_3$ glass system. *Ceram. Int.* **2021**, *47*, 27305–27315. [CrossRef]
30. Kilic, G.; Işsever, U.G.; Ilik, E. The synthesis and characterization of zinc-tellurite semiconducting oxide glasses containing Ta_2O_5. *Mater. Res. Express* **2019**, *6*, 065907. [CrossRef]
31. Tekerek, S. Calculation of Air Kerma of CT Contrast Agents and Painkiller. *J. Biomed. Res. Environ. Sci.* **2021**, *2*, 178–184. [CrossRef]